View metadata, citation and similar papers at core.ac.uk
brought to you by CORE
provided by Digital Repository @ Iowa State University

MEASUREMENT OF THE INDUCED MAGNETIC FIELD IN A FLAWED TUBE

J.A. Nyenhuis, J.C. Treece, and J.M. Drynan

Purdue University
School of Electrical Engineering
West Lafayette, IN 47907

H.A. Sabbagh

Sabbagh Associates
2634 Roundhill Lane
Bloomington, IN 47401

INTRODUCTION

In a standard eddy current method [1] for the inspection of tubing, a probe, consisting of two coils, is translated along the inside of the tube. Measured differences in impedance between the two coils are used to detect flaws in the wall of the tube. Physically what happens is alternating currents in the coils generate eddy currents in the wall of the tube. The magnetic field (primarily the axial component) from the eddy currents reduces the inductance of the coils from the free space values. A flaw will alter the eddy currents, resulting in a local change in magnetic field within the tube and hence a difference in impedance between the two coils.

Our goal in this work is to develop instrumentation for the gathering of data for the high resolution reconstruction [2,3] of flaws in nonferromagnetic tubing. To achieve this goal, a new probe and sensor assembly was developed. A solenoidal coil was used to generate an axially uniform exciting field inside the tube. The magnetic fields due to the eddy currents produced by the exciting field were measured by small magnetic field sensors which are located between the outside of the exciting coil and the inside wall of the tube. In an effort to obtain additional information on flaws inside the tube, all three components of the magnetic field were measured. This was done by suitable orientation of the magnetic sensors inside the tube. In this paper, we describe our instrumentation and present some experimental results.

EXPERIMENTAL PROCEDURE

A drawing of the exciting coil and sensor assembly is shown in Fig. 1. The exciting coil is a solenoid of length 6.3 cm and turns density 4000/m which is wound on a 0.5 inch diameter Teflon rod with a single layer of 32 AWG wire. A 50 Ω resistor is placed in series with the exciting coil to improve impedance matching with the coaxial cable that delivers current to the coil. The voltage across the 50 Ω terminator is monitored to determine the current through the exciting coil. The reac-

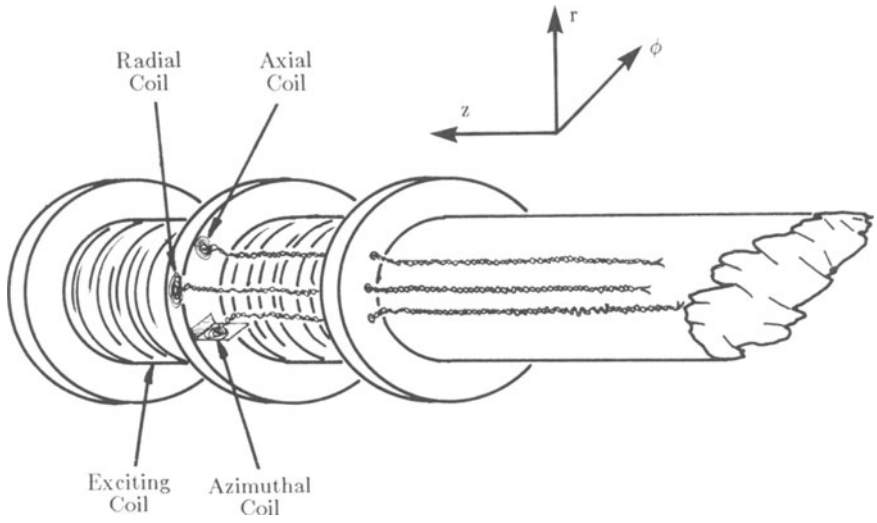

Fig. 1. Exciting coil and sensor assembly and co-ordinate definition.

tance of the exciting coil is primarily inductive for frequencies up to 10 MHz. The inductance was calculated to be 1.6×10^{-4} H in air and 10^{-4} H inside an unflawed region of the tube. Measurements of the inductance were in agreement with the calculations. On the outside of the exciting coil are located inductive pickup coils for the measurement of the magnetic field. The coils were wound in a single plane (hence the name, "pancake" coil [4]) to and insure that the coil is sensitive to only one component of the magnetic field and also to minimize capacitance. The coils consist of 5 turns of 36 AWG wire with an inner diameter of 0.4 mm and an outer diameter of 1.4 mm. The wires leading from the pick-up coils were tightly twisted to minimize the signal from the magnetic fields that are present along the length and in the vicinity of the exciting coil. By suitable orientation of the coils, the axial (B_z), radial (B_r), and azimuthal (B_ϕ) components of the magnetic field can be measured (see fig. 1 for a definition of the coordinates).

A block diagram of the experimental apparatus that was used is shown in Fig. 2. An HP 3312A function generator was used to generate a sinusoidal current in the exciting coil. The output voltage of the function generator was kept constant and the exciting coil current was 110 mA at 300 kHz. The exciting coil and sensor assembly was translated inside the tube with a laboratory micro-positioner with which measurements could readily be made at intervals of 0.01 inches. The exciting coil and probe assembly was manually rotated for measurements along the circumference of the tube. A custom lock-in amplifier was used to measure the field components in phase and in quadrature with the exciting coil current. For this amplifier, a DC output voltage of 1 volt represents an AC input of approximately 0.3 mV pp. An IBM Personal Computer with a Tecmar A-D board was used to gather the voltage data from the lock-in amplifier.

Measurements were made on a 304 stainless steel tube with a 7/8" inner diameter and a 0.048" wall thickness. Defects were manufactured inside the tube by Electro Discharge Machining (EDM). Cross-sectional diagrams of the flaws whose fields we report on here are shown in Fig. 3.

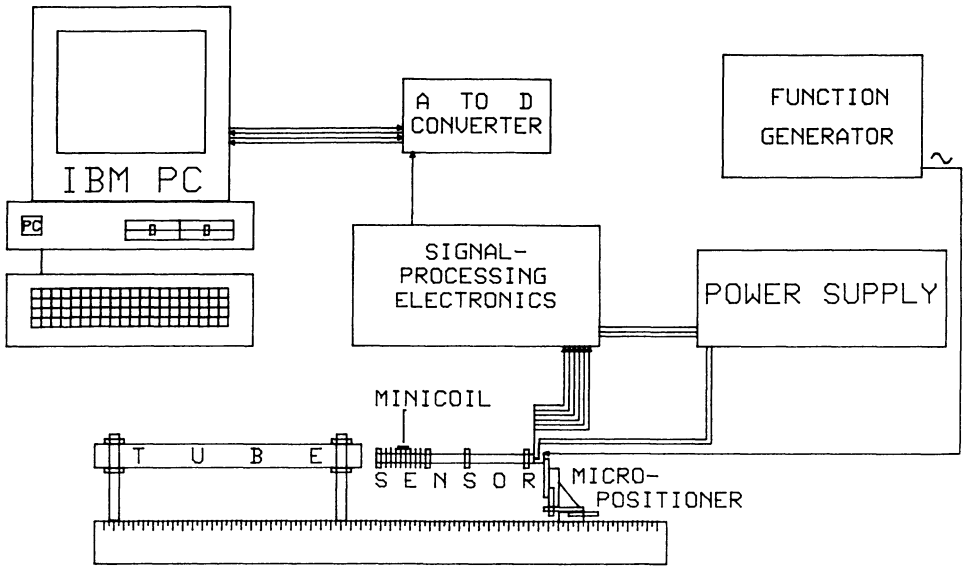

Fig. 2. Block diagram of the experimental apparatus.

SENSOR CHARACTERISTICS

It is of interest to qualitatively predict the sensitivity of the three orientations of the magnetic field sensor. In the unflawed tube, the eddy currents are circumferentially directed in the wall of the tube. This results in a magnetic field along the axis of the tube, i.e. in the z-direction. The radial and azimuthal field components are zero in the unflawed tube. A flaw in the form of a crack or a void causes a local reduction of the conductivity, leading to a reduction of the axial magnetic field and resulting in finite local radial and azimuthal magnetic field components.

We expect the axial sensor to provide a considerable magnetic field signal even in the absence of a flaw. The axial sensor essentially measures the magnetic field due to the eddy currents in the wall of the tube along the length of the solenoid. (Since the solenoid's length is much larger than its diameter, the magnetic field due to the current in the solenoid's windings is small compared to the field due to the eddy currents). In the presence of a flaw, we expect there to be a slight change in the axial signal since the flaw is expected to be of considerably smaller volume than the volume of tube wall in which the circumferential eddy currents flow.

The radial and axial sensors offer the advantage of there being no background signal in the absence of a flaw. From the inspection of fig. 1, it can be seen that the radial sensor measures the magnetic field closer to the wall of the tube than does either the axial or azimuthal sensor.

EXPERIMENTAL RESULTS

In order to demonstrate the nature of magnetic fields that arise from the different sensor orientations and also to obtain data for use in flaw reconstruction, the components of the magnetic field inside the tube were mapped in the vicinity of flaws. Some representative data are presented below.

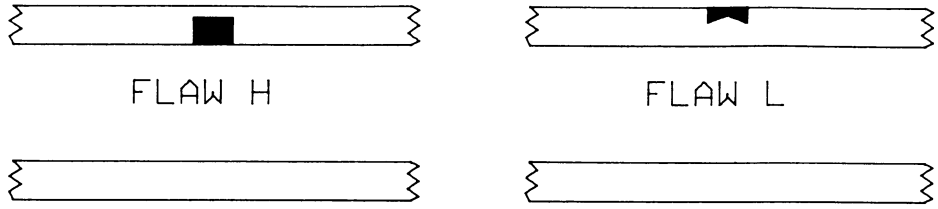

Fig. 3. Diagram of flaws H and L inside the 304 stainless steel tube. The tube has an inner diameter of 7/8" and a wall thickness of 0.048". Flaw H is a notch on the inner wall of length 0.2", width 0.022", and depth 0.0385". Flaw L is a doubly peaked notch on the outside wall of the tube of length 0.2", width 0.02", and depths 0.0235"/0.013".

Flaw H is a notch of depth 0.0385", width 0.022", and length 0.2" on the inside wall of the tube (see Fig. 3). In Fig. 4 we show the output voltage due to magnetic field components in the vicinity of flaw H. Plots labeled 90° in Figs. 4(a)-4(c) are for voltages in phase quadrature with the current in the exciting coil. Plots labeled 0° [Figs. 4(d) - 4(f)] are for voltages in phase with the exciting coil current. Flaw H is centered at z= 0.5" and $\phi = 0°$. In Fig. 4, an output signal of 1 V represents a peak-peak magnetic field of about 0.4 Oe.

The output voltage, V_{out}, due to the quadrature radial magnetic field component, B_r, for flaw H is shown in Fig. 4(a). Away from the flaw, B_r has a background signal of about 0.26V, probably due to stray pickup in the sensor leads. On the leading edge of the notch, at z=0.4", the radial signal decreases by about 0.15 V; on the trailing edge of the notch, at z=0.6", the radial signal is approximately 0.15V above the background level. There is no net radial signal, above the background level, at the center of the notch. V_{out} is rapidly reduced when the radial sensor is rotated away from the midline of flaw H. The reduction is about 50% for a sensor rotation of 5° at the leading and trailing flaw edges. The highest values of B_r are likely to be more localized in the azimuthal direction than is indicated in Fig. 4(a) since the radial sensor subtends an angle of about 8°.

The quadrature axial magnetic field component due to flaw H is shown in Fig. 4(b). In contrast with the case for the radial sensor, there now is a significant background signal of about -2.7 V. In the vicinity of the flaw, the field amplitude is reduced by about 0.07V. There are increases of approximately 0.03 V above the background in the amplitude of V_{out} at the leading and training edges of the flaw. The relative reduction of the signal due to B_z as the sensor is rotated inside the tube is similar to the reduction in the B_r signal.

The quadrature output voltage from the azimuthal magnetic field sensor for flaw H is shown in Fig. 4(c). The background signal level is similar to that of the radial sensor. The difference between the minimum and maximum flaw signal is about 0.1V, comparable to the net signal that was obtained from the axial sensor. There is some noise in the data, but it can be seen that B_ϕ is of opposite sign at adjacent corners of the notch and of the same sign at opposite corners.

The component of output voltage in phase with the exciting coil current, the 0° signal, was also measured in the vicinity of flaw H. The peak-to-peak output voltages of the 0° component of B_r, B_z, and B_ϕ were measured to be 0.05 V, 0.03V, and 0.02 V, respectively. These values are

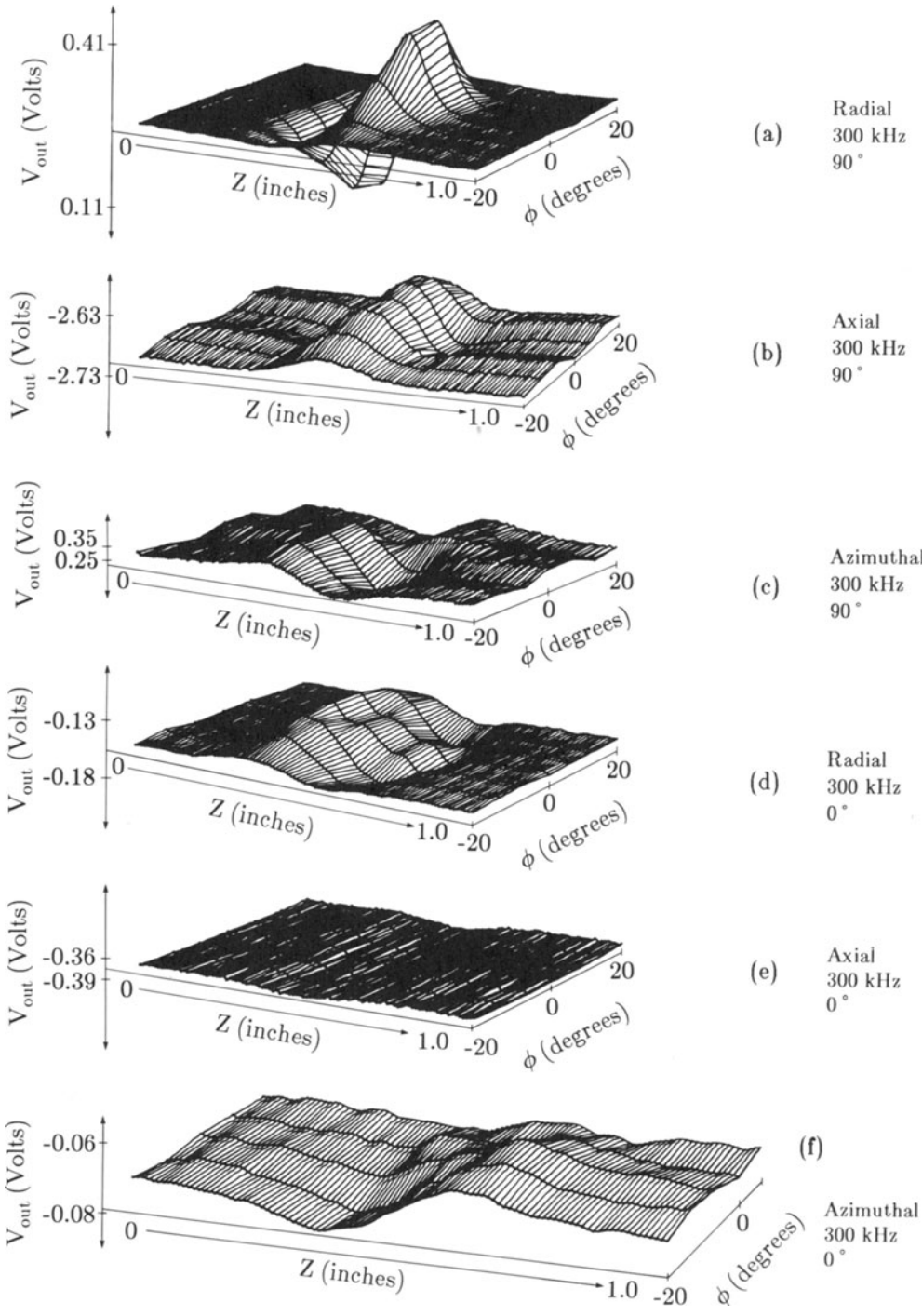

Fig. 4. Output voltages due to magnetic fields in the vicinity of flaw H. An output voltage of 1 V corresponds to a magnetic field of 0.4 Oe. The 90° voltage is in phase quadrature with the exciting coil current; the 0° voltage is in phase with the exciting coil current.

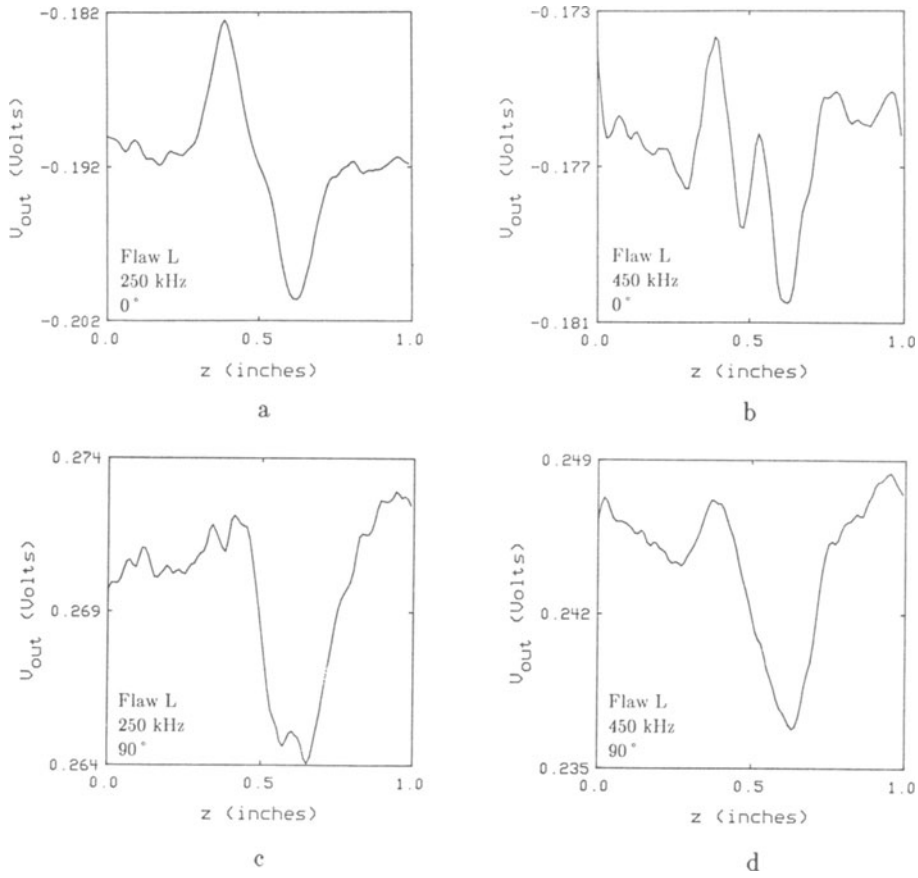

Fig. 5. Output voltages due to radial magnetic field sensor for flaw L at two different frequencies. The 0° and 90° signals are defined in the text.

less than the corresponding 90° voltages. A plot of V_{out} due to B_r in phase with the exciting coil current is shown in Fig. 4(d). This field map displays the odd symmetry about z=0.5" that is present in the plot of the 90° data in Fig. 4(a), and there are a few hills and depressions that are not present in Fig. 4(a). Insufficient signal strength for the 0° component of the axial and azimuthal field data [Figs. 4(e) and 4(f)] precludes a meaningful analysis of these field components.

Flaw L is a notch with two peaks on the outside wall of the tube (see Fig. 3). In Fig. 5 are shown the radial field data for flaw L for frequencies of 250 kHz and 450 kHz. The frequency was varied in order to illustrate the effects of the skin depth on the output signal. The influence of the two peaks of flaw L can be seen by comparing the 250 kHz and 450 kHz 0° data in Figs. 5(a) and 5(b). At 250 kHz, the skin depth is calculated to be 0.033" and the probe essentially "sees" flaw L as a single entity. There is a single maxima and minimum in V_{out} when the probe is moved past the flaw which is centered at z=0.5" [Fig. 5(a)]. At 450 kHz, the skin depth is calculated to be 0.024" and the probing field "sees" more of the two peaks of the flaw than the part adjacent to the tube's outer wall. This is evidenced by the existence of two maxima and minima in the output voltage as the probe is moved past the flaw [Fig. 5(b)]. The output signals in phase quadrature with the exciting coil current are shown in Figs. 5(c) and 5(d). V_{out} for the 90° data is frequency depen-

dent, but the effect of the different frequencies is not as readily explained as it is for the 0° data. The 250 kHz, 90° data exhibits the curious effect of not being symmetric about the flaw center. Determining if this is a real effect or an experimental anomaly requires further investigation.

The output voltages due to flaw L are considerably less than those due to flaw H. The fact that the flaw is on the outside of the tube means that less of the exciting current reaches it, and it also results in a reduction of the field reaching the sensor. For flaw L, the 0° output signal is of comparable magnitude to the 90° signal. This may be due to the fact that this flaw is on the outside of the tube.

The magnetic fields analogous to the experimental results in Fig. 4 were calculated by an integral solution using a Green's function for a cylinder together with a discretized model of flaw H [2,3]. The symmetries in the experimental data were corroborated by the calculation as were other qualitative features of the experimental data. There were, however, some quantitative discrepancies between experiment and calculation and these are being investigated.

DISCUSSION

The form and symmetry of the magnetic field components in the vicinity of flaw H can be deduced by simple arguments. Consider a slot of length L in an otherwise uniform conducting sheet. Let the co-ordinate system origin be centered inside the slot with y=0 being at the surface of the conducting sheet (see Fig.6). Assume that the current density, $\underline{J}$, per unit length is $J_0\hat{\underline{x}}$ far away from the slot. This current produces a magnetic field $\underline{B} = \mu_0 J_0 \hat{\underline{z}}/2$. In the vicinity of the slot we write the current density as $\underline{J} = \underline{J_0}\hat{\underline{x}} + \underline{J_i}$. The slot is effectively creates a dipole current source which produces an "image" current density, J_i. Inside the slot, where there is no conducting material, $\underline{J_i} = -J_0\hat{\underline{x}}$.

In the vicinity of the slot, the magnetic field has non-vanishing z and y components. B_y attributable to the image current within the slot has amplitude maxima at the leading and trailing edges of the slot ($z = \pm L/2$; x,y=0) and is negative at z=-L/2, positive at z=+L/2, and is 0 at z=0. B_z due to the image current within the hole has an amplitude maximum at the co-ordinate origin and opposes the uniform magnetic field that would be present in an unflawed sheet. The image circulation currents at the leading and trailing slot edges produce fields that enhance B_y due to the image current in the slot. The image circulation currents outside the

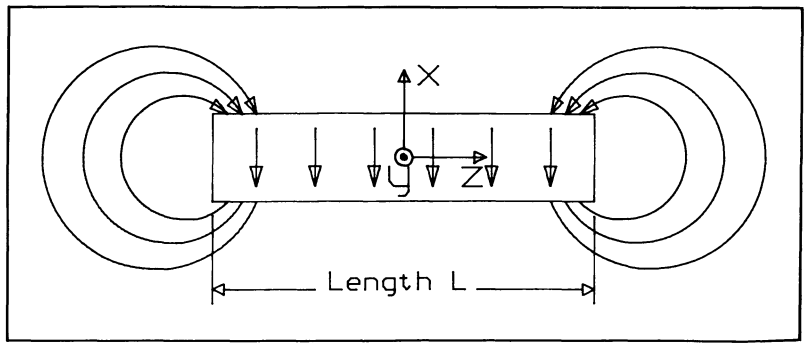

Fig. 6. Schematic diagram of the image currents due to a slot in a large sheet of current.

slot produce a positive z component of magnetic field. We expect therefore that B_z will have a minimum above the center of the slot and local maxima near the leading and trailing slot edges. The image circulation currents have a non-zero z component near the corners of the slot, resulting in a non-zero B_x in the vicinity of the corners of the slot. The sign of B_x is opposite for adjacent corners and the same for opposing corners.

The magnetic fields due to flaw H in Fig. 4 are qualitatively explained by noting that the x,y,z directions in the infinite sheet co-ordinates are analogous to the ϕ, r, and z co-ordinates inside the tube.

As is suggested above, the radial and azimuthal data offer the advantage of providing a signal only in the presence of a flaw whereas the B_z is significant even in the absence of a flaw. As is seen from the data and the above qualitative argument, the radial signal is strongest at the leading and trailing edges of the flaw. The axial signal is strongest at the center of the flaw. The two weak maxima near the ends of the slot in the axial signal in Fig. 4 also provide information on the location of the flaw's edges. The azimuthal signal is the strongest at the corners of the flaw. Thus, it can be said that each component of the magnetic field provides a different type of information on the flaw.

The fact that the radial sensor can be brought close to the wall of the tube offers advantages for this sensor orientation over the z and ϕ sensors. A straightforward calculation shows that the normal magnetic field component at the edge of a hole in a current carrying sheet is a rapidly decreasing function of increasing distance above the surface of the sheet [5]. It is therefore important to bring the radial sensor as close as possible to the wall of the tube. The significant perpendicular magnetic fields that exist at the edges of holes in current carrying sheets find technological application elsewhere as well; this effect is used to constrain magnetic bubbles in a current access bubble memory [5].

ACKNOWLEDGEMENTS

The flawed tube was furnished by Susan N. Vernon, Code R34, Naval Weapon Support Center, White Oak Labs, Silver Spring, MD. This work was supported by Sabbagh Associates. Work at Sabbagh Associates was supported by Department of Energy Contract No. DE-AC02-83ER80096. We thank L. David Sabbagh for the calculation of the magnetic fields and plotting of the results.

REFERENCES

1. C. Rose, IEEE Trans. Magn. Mag-20, 1983 (1984).
2. H.A. Sabbagh and L.D. Sabbagh, "Development of an Eddy Current Sensor and Algorithm for Three Dimensional Quantitative Non-Destructive Evaluation", Phase I Final Report on Contract # DE-AC02-83ER80096 between Department of Energy and Sabbagh Associates, 27 February 1984.
3. L.D. Sabbagh and H.A. Sabbagh, Review of Progress in Quantitative Nondestructive Evaluation, vol. 4a, p. 635, edited by D.O. Thompson and D.E. Chimenti, Plenum Press, New York, 1984.
4. K. Ju and F.B. Humphrey, J. Appl. Phys. 48, 4656 (1977).
5. A.H. Bobeck, S.L. Blank, A.D. Butherus, F.J. Ciak, and W. Strauss, Bell Syst. Tech. J. 58, 1453 (1979).